Journal of Applied Electrochemistry (2006) 36:663–668
DOI 10.1007/s10800-006-9118-y

Preparation and characterization of TiO_2/Ti film electrodes by anodization at low voltage for photoelectrocatalytic application

Y.B. XIE and X.Z. LI*
Department of Civil and Structural Engineering, The Hong Kong Polytechnic University, Hong Kong, China
*(*author for correspondence, tel.: +86-852-2766-6016, fax: +86-852-2334-6389, e-mail: cexzli@polyu.edu.hk)*

Received 15 August 2005; accepted in revised form 4 January 2006

Key words: anodic oxidation, anodization, bisphenol A, BPA, oxidation, PEC, photoelectrocatalytic, Ti, TiO_2, titanium, titanium dioxide

Abstract

Multiporous TiO_2/Ti film electrodes were prepared by different anodic oxidation processes at low voltage, in which the micro-structured TiO_2 thick films were prepared in H_2SO_4–H_2O_2–H_3PO_4–HF solution for 2 h and the nano-structured TiO_2 thin films were prepared in H_3PO_4–HF solution for 30 min with post-calcination. Both types of TiO_2/Ti films were characterized by scanning electron microscopy and X-ray diffraction analysis. The photocatalytic (PC) and photoelectrocatalytic (PEC) reactivity of the TiO_2/Ti electrodes were evaluated in terms of bisphenol A (BPA) degradation in aqueous solution. The experimental results demonstrated that the nano-structured TiO_2/Ti thin-film electrodes had higher reactivity in the BPA degradation reaction. The PEC degradation of BPA was further studied using different cathodes, either a reticulated vitreous carbon (RVC) electrode or a platinum (Pt) electrode. The experimental results confirmed that the efficiency of BPA degradation could be significantly enhanced in the TiO_2/Ti–RVC reaction system due to the generation of H_2O_2 on the RVC cathode. It is believed that such a H_2O_2-assisted TiO_2 PEC oxidation process may have good potential for water and wastewater treatment.

1. Introduction

Photoreactive materials have received much attention due to their inherent photochemical properties. Titanium dioxide or titania (TiO_2) is a particularly-versatile semiconductor with a variety of applications in photocatalysis such as gas sensors, photovoltaic cells, optical coatings, structural ceramics and biocompatible materials [1, 2]. It has been confirmed that the architecture of titania can greatly influence its physiochemical properties [3]. Although many techniques including sol-gel, precipitation–peptization, hydrothermal synthesis and electrochemical methods etc. have been developed to produce various nano-structured titania powders with better photoactivity [4–6], most immobilized TiO_2 films are usually prepared by a dip-coating method on different supporting media. These films showed a limit to promote their photoelectrocatalytic activity due to a low rate of electron transfer between the TiO_2 film and its supporting materials.

Alternatively, anodic oxidation of titanium (Ti) metal in acidic solution by applying an electrical current between a Ti electrode and a counter electrode is an effective process to prepare a TiO_2 film. Such a TiO_2/Ti films as a photoelectrode has several advantages over other TiO_2 films, due to an efficient mass transfer between TiO_2 layer and Ti metal for driving electrons away from the TiO_2 surface. In addition, the thickness and morphology of such TiO_2 films are easily controlled by regulating electrical potential/current or chemical composition of electrolyte solution. The high-voltage anodization process has been intensively studied and applied to prepare the crystallized TiO_2 film without any thermal treatment [7, 8]. However, these anodized TiO_2 films usually have a detached-hole structure at a scale of micrometers, resulting from a violent electrolyzing oxidation reaction at a high anode–cathode voltage (usually above 160 V) far beyond a sparking discharge voltage (about 100 V) [8–10].

This study aims at developing a low-voltage anodization process to prepare some well-crystallized TiO_2/Ti films with a smaller pore size. The prepared TiO_2/Ti films will be characterized and their photocatalytic (PC)/photoelectrocatalytic (PEC) activity will be evaluated in the degradation of bisphenol A (BPA), as a model endocrine disrupter, in aqueous solution under UV illumination.

2. Experimental

2.1. *Preparation of TiO_2/Ti film electrodes*

Titanium sheets (purity: 99.6%; thickness: 0.14 mm) from Goodfellow Cambridge Ltd. were used as a raw

material to prepare the TiO_2/Ti film electrodes. A piece of Ti sheet (1×5 cm) was ultrasonically cleaned in alcohol and acetone solutions, respectively and then washed with distilled water. The cleaned Ti sheet was submerged in 2 M HF solution for 2 min to polish its surface chemically.

An anodic oxidation process was conducted in a dual-electrode reaction chamber, in which the cleaned Ti sheet was used as the anode and a Pt foil of the same size was applied as the cathode. Two electrodes were submerged in a mixture of electrolyte solution and a direct-current electrophoresis power supply (EPS 600) was used to provide different electrical potentials/currents between two electrodes during the anodic oxidation reaction. The TiO_2/Ti film electrodes were prepared by two different processes:

Process A: Low-voltage (20–40 V) and long-time (6 h) anodization in aqueous H_2SO_4(1.0 M)–H_3PO_4(0.3 M)–H_2O_2 (0.6 M)–HF(0.03 M) solution.

Process B: Low-voltage (10–50 V) and short-time (30 min) anodization in aqueous H_3PO_4(0.5 M)–HF(0.1 M) solution plus post-calcination at 723 K for 2 h.

2.2. *Characterization of TiO_2/Ti film electrodes*

To study the surface morphology, average pore size, and pore distribution, the TiO_2/Ti films were examined by scanning electron microscopy (SEM LEO Stereoscan 440) equipped with an energy dispersive X-ray (EDX) facility (Oxford ISIS). To determine the crystal phase composition, X-ray diffraction (XRD) measurement was carried out using a diffractometer (Philips PW3020) fitted with a graphite monochromator. An accelerating voltage of 40 kV and a current of 30 mA were used to produce Cu K_α radiation at a wavelength of 0.15418 nm.

2.3. *Experimental setup*

A bench-scale photoreaction system consisted of a cylindrical quartz glass reactor with a standard three-electrode configuration and an 8-W medium-pressure mercury lamp (LZC-UVA-365) with a main emission at 365 nm as an external UV-A light source. A TiO_2/Ti film electrode was positioned at the bottom of the reactor as the photoanode and a Pt or RVC counter electrode was placed nearby a gas diffuser as the cathode. A saturated calomel electrode (SCE) was also used as the reference electrode. The electrical potential and current on the electrodes were controlled by a potentiostat–galvanostat (ZF-9). The photoelectrochemical experiments were performed in a constant anodic potential mode.

2.4. *Analytical methods*

The BPA concentration was analyzed by high-performance liquid chromatography (Finnigan LCQ DUO). A reversed phase column (Atlantis d-C18, 150×4.6 mm ID, 5 μm beads) and a mobile phase of acetonitrile/water (70/30 V/V) at a flow rate of 0.8 ml min^{-1}, were used for BPA separation. A UV detector (UV6000LP) was used to determine BPA concentration at 278 nm.

3. Results and discussion

3.1. *SEM analysis*

The first TiO_2/Ti film sample was prepared by Process A at 40 V for 6 h and its surface morphology was examined by SEM. Two SEM images of this TiO_2/Ti film sample are shown in Figure 1. Figure 1(a) shows that a TiO_2/Ti film was formed with a multiporous structure with the aggregated particles on its surface. The average sizes of individual particles and micropores were found to be at a low side of micrometer scale. The lateral morphology was also measured by cross-sectional SEM observation. Figure 1(b) shows that a TiO_2 film was directly formed on the Ti medium by anodization, successfully, exhibiting an alveolar hole structure. The thickness of this TiO_2 film was determined to be about 4 μm. These results indicate that Process A with long-time anodization would form a thick and microstructured TiO_2 layer, which would be beneficial to

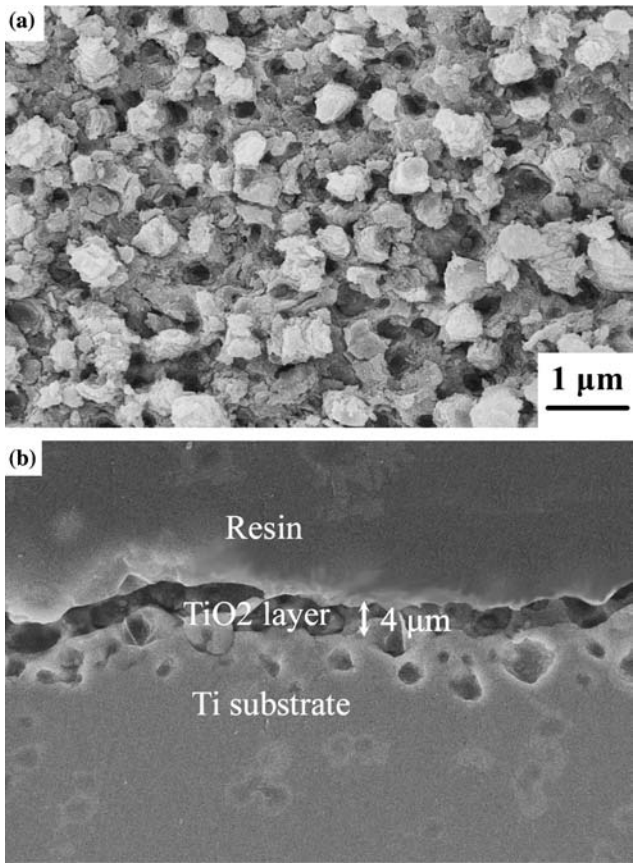

Fig. 1. (a) SEM and (b) cross-sectional images of TiO_2/Ti thick-film electrode fabricated by Process A (anodization at 40 V for 6 h).

interfacial adsorption of organic substrate from aqueous phase.

The second TiO_2/Ti film electrode was prepared by Process B at 30 V for 30 min with post-calcination at 723 K for 2 h. Its SEM images are shown in Figure 2. Figure 2(a) shows that a nano-structured TiO_2 thin film with a cross-linked multiporous network structure was formed on the Ti medium. The average size of individual holes was found to be about 50 nm and interconnection wall thickness was around 30 nm in average. The thickness of this TiO_2 layer was about 650 nm by cross-sectional SEM observation as shown in Figure 2(b). These results demonstrate that Process B with short-time anodization produced a much thinner TiO_2 film than Process A, which means the growth of TiO_2 film on the Ti medium can be well controlled by an anodizing time. These findings are in agreement with the results in other research [11]. It is generally believed that a heterogeneous photocatalytic reaction in aqueous solution mainly occurs on the interface of solid catalysts and dissolved compound molecules. Furthermore, the photocatalytic reactivity of a well-crystallized TiO_2 film mostly depends on its mass-transfer and light-transfer efficiency, depending on the solid–liquid contacting area and UV photons transiting area. Some research has confirmed that the increase of TiO_2 film thickness does not always lead to a corresponding enhancement of photoactivity once a TiO_2 film reaches a certain thickness [12].

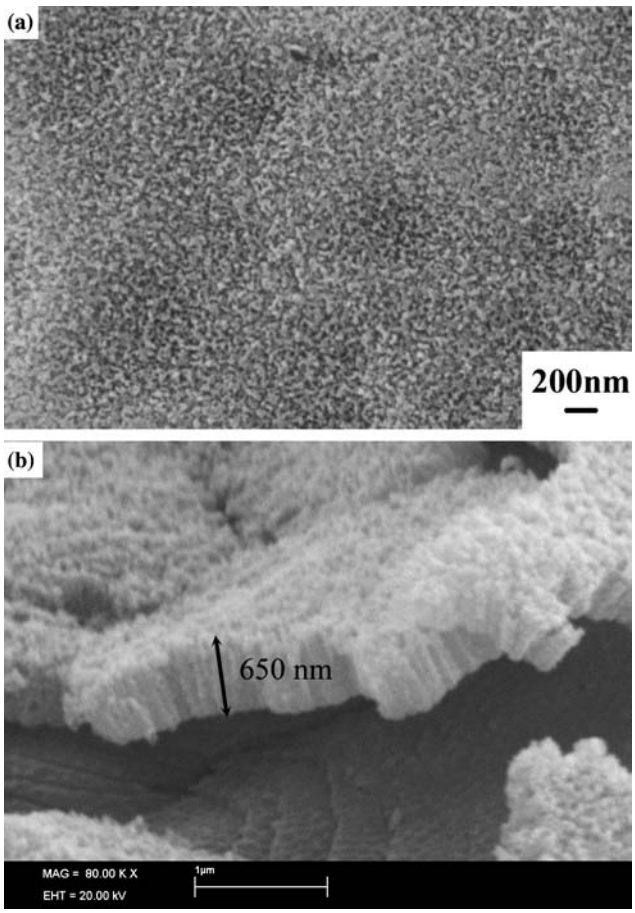

Fig. 2. (a) SEM and (b) cross-sectional images of TiO_2/Ti thin-film electrode fabricated by Process B (anodization at 30 V for 30 min plus post-calcination).

3.2. *XRD analysis*

Three micro-structured TiO_2/Ti thick-film electrodes were prepared by Process A at different voltages of 20, 30, and 40 V, respectively, and examined by XRD. Their XRD patterns are shown in Figure 3. The XRD patterns show that all TiO_2/Ti samples only exhibited an anatase phase and confirmed that Ti metal in the H_2SO_4(1.0 M)–H_3PO_4(0.3 M)–H_2O_2 (0.6 M)–HF(0.03 M) solution was successfully anodized to TiO_2 with a well-crystallized structure in Process A at the low voltage. The results further indicate that the anodic oxidation reaction by applying electrical potential at a higher voltage could be beneficial to achieve a higher degree of TiO_2 crystallization. Among them, the TiO_2/Ti film electrode formed at 40 V had the most regular crystal structure of an anatase phase. It should be noticed that this process lasted for 6 h.

To further study the above anodization process at a low voltage for a short anodizing time, two more TiO_2/Ti films were prepared in H_3PO_4 (0.5 M)–HF(0.1 M) solution by Process B at 30 V for 30 min only. One was further calcined at 723 K for 2 h, while the other was not heated. Their XRD patterns are shown in Figure 4. It was found that the nano-structured TiO_2 thin film formed at 30 V for 30 min without calcination had mainly an amorphous structure due to a very short anodizing time. However, after calcination at 723 K for 2 h, a well-crystallized TiO_2 film with an anatase-dominated structure was formed. These results indicate that either a long-time anodization without further thermal treatment or a short-time anodization with post-calcination can form the well-crystallized TiO_2 films successfully.

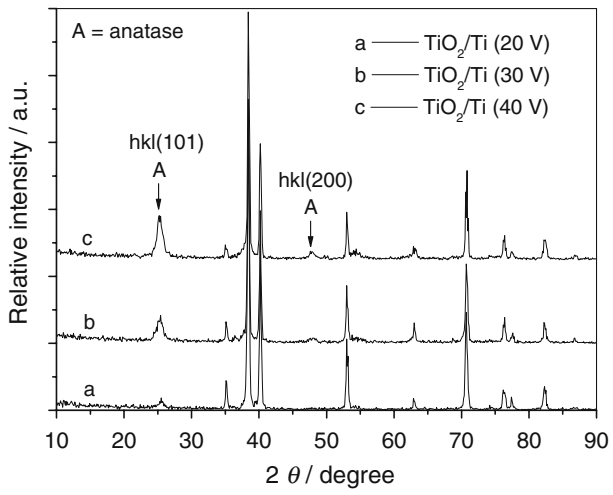

Fig. 3. XRD patterns of TiO_2/Ti thick-film electrodes prepared by Process A (anodization at 20, 30 and 40 V, respectively for 6 h).

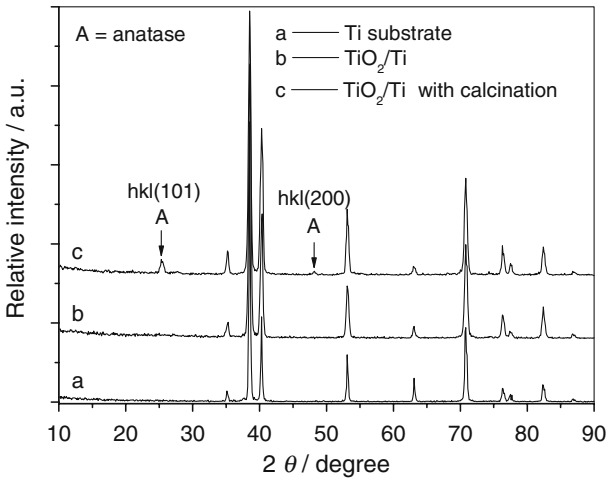

Fig. 4. XRD patterns of TiO_2/Ti thin-film electrodes prepared by Process B (anodization at 30 V for 30 min).

During the above anodization process, titanium metal in aqueous acidic solution could be oxidized into various oxides such as TiO_2 and Ti_2O_3 with different valence states, as long as the positive potential applied on the titanium anode was higher than its theoretical oxidation potentials (1.630 V for Ti/Ti^{2+}; 1.998 V for Ti/Ti^{3+}; 2.188 V for Ti/Ti^{4+} vs SCE). At a higher potential, titanium metal would be transferred into TiO_2 more completely. On the other hand, there existed a competition between an oxidation reaction to form TiO_2 ($Ti + 2H_2O \rightarrow TiO_2 + 4H^+$) and a dissolution reaction to release titanium ions from TiO_2-electrolyte interface into the bulk solution ($TiO_2 + 6HF \rightarrow [TiF_6]^{2-} + 2H_2O + 2H^+$ and $TiO_2 + H_2O + H^+ \rightarrow [Ti(OH)_3]^+$). Furthermore, a side reaction to generate oxygen from water ($2H_2O - 4e^- \rightarrow O_2 + 4H^+$) also occurred on the TiO_2/Ti anode.

The above results confirmed that titanium metal can be successfully anodized to TiO_2 in both electrolyte solutions at the low voltage. However, the TiO_2 crystallization without thermal treatment needed a longer time to approach, in which the H_2O_2 in the H_2SO_4–H_2O_2–H_3PO_4–HF solution played a positive role in shortening the process time ($2Ti + 2H_2O + H_2O_2 \rightarrow 2TiO_2 + 6H^+$). In summary, the voltage applied at the titanium anode, the anodizing time and the composition of electrolyte solution are three key factors to control the surface morphology and crystal structure of the product TiO_2/Ti films significantly.

3.3. *Photoelectrochemical measurement of TiO_2/Ti film electrodes*

To study the photoelectrochemical properties of the anodized TiO_2/Ti film electrodes, a set of linear sweep voltammogram measurements with and without UV illumination was conducted in 0.01 M Na_2SO_4 solution using three different anodes: (a) a nano-structured TiO_2/Ti electrode prepared by Process B; (b) a micro-structured TiO_2/Ti electrode prepared by Process A; and (c) a Ti metal electrode. The analytical results as *I–V* curves are presented in Figure 5.

It can be seen that the *I–V* curve of Ti metal electrode (curve "c") in the dark demonstrated a typical metal anodization behavior. The anodic current increased very slowly at the low voltage range and then began to increase continuously over a critical oxidation potential of water due to oxygen evolution. When this electrolyzing voltage was further increased above the critical oxidation potential of Ti, a sharp enhancement of anodic current occurred, resulting from a titanium metal oxidation reaction along with a water-splitting reaction.

Two *I–V* curves of TiO_2/Ti electrodes in the dark (curves "A" and "B") showed that their critical dielectric breakdown potentials were about 3 V. This result demonstrated a typical character of *n*-type semiconductor, where a large anodic current only occurs over a breakdown potential. Obviously, this anodic current of the TiO_2/Ti electrode should be derived from not only the reaction of oxygen evolution, but also anodic dissolution of TiO_2 electrode itself. However, the latter effect plays an insignificant role when the applied potential is below the electric breakdown potentials of the TiO_2/Ti electrode. This phenomenon is different from that of the Ti metal electrode.

Compared to the results in the dark, the *I–V* curves of TiO_2/Ti electrodes under UV illumination (curves "a" and "b") demonstrated that the significant response of anodic current appeared under UV illumination. However, the nano-structured TiO_2/Ti electrode exhibited the higher current response than the micro-structured TiO_2/Ti electrode at the same anodic potential. It should be noted that a total response of anodic currents was combined with a photocurrent and an electrochemical current. While the electrochemical current results from the water oxidation on the TiO_2/Ti anode, the photocurrent should result from a regular transfer of TiO_2 conduction band electrons excited by UV irradiation.

It is well known that the most photo-induced electro-hole pairs (e^-–h^+) could be recombined quickly,

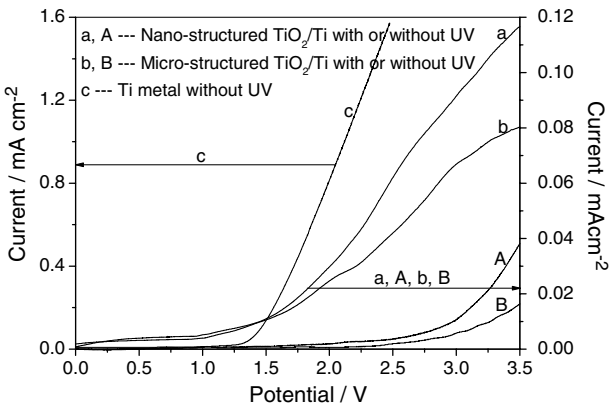

Fig. 5. Linear sweep voltammogram curves of (a) nano-structured TiO_2/Ti electrode (b) micro-structured TiO_2/Ti electrode (c) Ti metal sheet in 0.01 M Na_2SO_4 solution in the dark or UV illumination.

although TiO_2 electrons can be easily excited from the valence band to the conduction band by UV excitation. In such a PEC reaction system, externally applied anodic potential on the TiO_2/Ti electrode could drive the photo-induced electrons from the TiO_2 conduction band to form an external circuit current and enhance the e^-–h^+ separation. However, the overall efficiency of electron transfer through a TiO_2/Ti electrode depends highly on the surface micro-structure of TiO_2 films and its supporting material, which influences the electron-transition inside the semiconductor and electron-transfer on the interface of the TiO_2/Ti electrode [13]. Apparently, the experimental results in this study demonstrate that the higher anodic potential caused the higher current response and a significant photocurrent response occurred when the applied potential was above 1.5 V vs SCE. However, to avoid significant anodic corrosion (or dissolution) of the TiO_2/Ti electrode itself, the potential applied was controlled at 3.0 V vs SCE only in the following experiments.

3.4. *PC activity of TiO_2/Ti film electrodes for BPA degradation*

Both the micro-structured TiO_2/Ti thick-film electrode prepared by Process A and the nano-structured TiO_2/Ti thin-film electrode prepared by Process B were applied for PC reaction. A set of experiments was conducted in aqueous BPA solution with an initial BPA concentration of 11.2 mg l^{-1} and pH 6.17. The reaction solutions were diffused using different gases at a flow rate of 120 ml min^{-1}. The experimental results of BPA degradation are shown in Figure 6. It can be seen that the photoreactivity of the micro-structured TiO_2/Ti electrode was gradually enhanced by different aerations from nitrogen to air and further to oxygen, resulting from the superior capability of dissolved oxygen molecules to scavenge TiO_2 conduction-band electrons. Furthermore, the experimental results of BPA degradation in the oxygen-diffused PC reaction demonstrate that the nano-structured TiO_2 thin film performed better (BPA removal = 88%) than the micro-structured TiO_2 thick film (BPA removal = 76%).

It should be noted that the surface morphology of an anatase TiO_2 film significantly affects its responsive photocurrent as well as photoreactivity, since heterogeneous photochemical reaction mainly occurs on the interfacial surface of catalysts and reactants [14]. The nano-structured TiO_2/Ti thin film revealed a higher PC activity than the micro-structured TiO_2/Ti thick film due to a finer porous structure and a higher degree of crystallization. Hence the nano-structured TiO_2 multi-porous film could provide much larger contact area for BPA adsorption and UV photon transmission in comparison with the micro-structured TiO_2 thick film in such a heterogeneous reaction system. Therefore, it is confirmed that the photocatalytic reactivity of a TiO_2/Ti film electrode depends on the morphology of surface micro-structure and degree of crystallization rather than its film thickness under this experimental condition [12].

3.5. *PEC activity of TiO_2/Ti film electrodes for BPA degradation*

The BPA degradation in the PEC reaction was also investigated using both the micro-structured and nano-structured TiO_2/Ti electrodes, respectively. In the PEC reaction, the TiO_2/Ti electrode was used as the anode and the RVC or Pt electrode was used as the cathode. A constant potential of 3.0 V vs SCE was applied in all experiments. Aqueous BPA solution was prepared with an initial concentration of 11.2 mg l^{-1}, an initial pH 6.17 and 0.01 M Na_2SO_4.

The first set of electrolysis reaction tests was carried out for BPA degradation in the dark. The experimental results are presented in Figure 7 as curves "a", "b" and "c". It can be seen that the overall removals of BPA after 180 min in the dark were only 5% for the micro-structured TiO_2/Ti electrode, 5% for the nano-structured

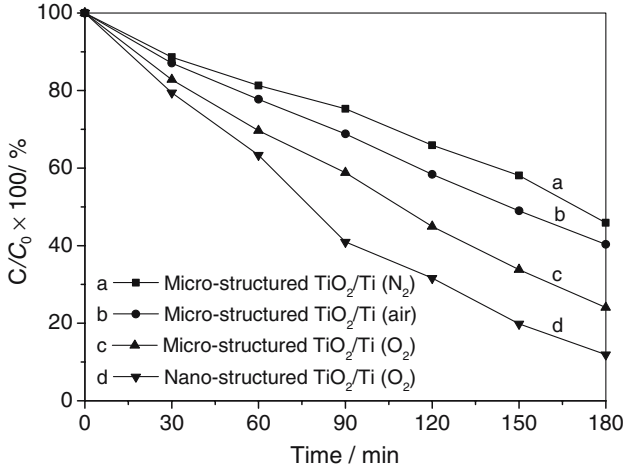

Fig. 6. Temporal BPA degradation ratio by the process of photocatalytic oxidation.

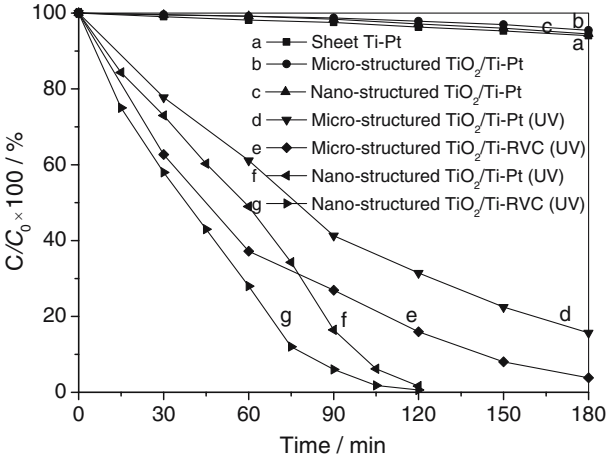

Fig. 7. Temporal BPA degradation ratio by the processes of electro-oxidation and photoelectrocatalytic oxidation (anode potential constant at 3.0 V vs SCE).

TiO_2/Ti electrode and 6% for the Ti electrode. These results indicate that the electrochemical oxidation played a minor role in this reaction. Consequently, the second set of experiments was conducted under the same condition but with UV illumination. The experimental results are also presented in Figure 7 as curves "d", "e", "f" and "g". These experiments demonstrated the significant enhancement of BPA degradation under UV illumination. The overall removals of BPA using the micro-structured TiO_2/Ti electrode were 76% in the TiO_2–Pt PEC reaction and 84% in the TiO_2–RVC PEC reaction after 180 min. Similarly, the overall removals of BPA using the nano-structured TiO_2/Ti electrode were 84% in the TiO_2–Pt PEC reaction and 96% in the TiO_2–RVC PEC reaction after 120 min.

It is clear that the nano-structured TiO_2/Ti thin-film exhibited the higher BPA degradation efficiency than the micro-structured TiO_2/Ti thick-film electrode at the same anodic potential in both configurations of TiO_2–Pt and TiO_2–RVC. Furthermore, all experiments confirmed that the BPA degradation in the TiO_2–RVC system was more efficient than that in the TiO_2–Pt systems. This indicates that under the same experimental conditions, using a RVC cathode to replace a normal Pt cathode could improve the BPA degradation significantly without extra operating costs. It is believed that the enhanced reaction in the TiO_2–RVC system results from the promoted generation of hydroxyl radicals ($H_2O_2 + e^-_{(CB)} \rightarrow \cdot OH + OH^-$) due to H_2O_2 production on the RVC cathode ($O_2 + 2H_2O + 2e^- \rightarrow 2H_2O_2$) as a H_2O_2-assisted TiO_2 photocatalysis. It can be noted that the applied electrical current in the above experiments was quite low at the anodic potential of 3.0 V. As a result, the real ability of the RVC electrode to generate H_2O_2 in such a dual-electrode TiO_2 PEC reaction system has not been fully reflected. A three-electrode reaction system is being studied by our group to further promote the H_2O_2 generation on the RVC electrode.

4. Conclusions

Crystalline micro-structured TiO_2/Ti thick-film electrodes can be prepared by long-time anodization at a low voltage without subsequent calcination. Crystallized nano-structured TiO_2/Ti thin-film electrodes can be prepared by short-time anodization at low voltage with post-calcination. The BPA degradation experiments using both electrodes demonstrated that the photocatalytic reactivity of the TiO_2/Ti electrodes depended mainly on their surface morphology and crystal structure rather than their film thickness, and the nano-structured TiO_2/Ti thin-film electrode was more efficient than the micro-structured thick-film electrode. The experiments also confirmed that the efficiency of BPA degradation can be further increased significantly by using a RVC cathode instead of a Pt cathode.

Acknowledgements

We thank the Hong Kong Government Research Grant Committee for financial support to this work (RGC No: PolyU5148/03E). We also thank Mr. Simon Y. Li for English proofreading.

References

1. A. Fujishima, T.N. Rao and D.A. Tryk, *Electrochimica ACTA* **45** (2000) 4683.
2. M. Gratzel, *Nature* **414** (2001) 338.
3. O.K. Tan, W. Cao, Y. Hu and W. Zhu, *Ceram. Int*. **30** (2004) 1127.
4. I.M. Arabatzis, S. Antonaraki, T. Stergiopoulos, A. Hiskia, E. Papaconstantinou, M.C. Bernard and P. Falaras, *J. Photochem. Photobiol. A-Chem*. **149** (2002) 237.
5. G.R. Reddy, A. Lavanya and C. Anjaneyulu, *Bull. Electrochem*. **20** (2004) 337.
6. S. Hore, E. Palomares, H. Smit, N.J. Bakker, P. Comte, P. Liska, K.R. Thampi, J.M. Kroon, A. Hinsch and J.R. Durrant, *J. Mater. Chem*. **15** (2005) 412.
7. R. Beranek, H. Hildebrand and P. Schmuki, *Electrochem. Solid State Lett*. **6** (2003) B12.
8. J.S. Choi, R.B. Wehrspohn, J. Lee and U. Gosele, *Electrochim Acta* **49** (2004) 2645.
9. S.K. Poznyak, D.V. Talapin and A.I. Kulak, *J. Electroanal. Chem*. **579** (2005) 299.
10. Y.T. Sul, C.B. Johansson, Y. Jeong and T. Albrektsson, *Med. Eng. Phys*. **23** (2001) 329.
11. V. Zwilling, E. Darque-Ceretti, A. Boutry-Forveille, D. David, M.Y. Perrin and M. Aucouturier, *Surf. Interface Anal*. **27** (1999) 629.
12. A. Danion, J. Disdier, C. Guillard, F. Abdelmalek and N. Jaffrezic-Renault, *Appl. Catal. B-Environ*. **52** (2004) 213.
13. F.Y. Oliva, L.B. Avalle, E. Santos and O.R. Camara, *J. Photochem. Photobiol. A-Chem*. **146** (2002) 175.
14. J. Rostalski and D. Meissner, *Sol. Energy Mater. Sol. Cells* **63** (2000) 37.